

# When can localized spins interacting with electrons in ferro- or antiferromagnets be described classically via the Landau-Lifshitz equation: Transition from quantum many-body entangled to quantum-classical nonequilibrium states

Priyanka Mondal and Branislav K. Nikolić\*

*Department of Physics and Astronomy, University of Delaware, Newark, DE 19716, USA*

Typical experiments in spintronics and magnonics operate with very large number of localized spins within ferromagnetic (FM) or antiferromagnetic (AFM) materials, so that their nonequilibrium dynamics is standardly described by the Landau-Lifshitz (LL) equation treating localized spins as classical vectors of fixed length. However, spin is a genuine quantum degree of freedom, and even though quantum effects become progressively less important for spin value  $S > 1$ , they exist for all  $S < \infty$ . While this has motivated exploration of the limits of applicability of the LL equation, by using examples of FM insulators and comparing LL trajectories to quantum expectation values of localized spin operators, analogous comparison of fully quantum many-body vs. quantum-for-electrons-classical-for-localized-spins dynamics in systems where *nonequilibrium* conduction electrons are present is lacking. Here we employ quantum Heisenberg FM or AFM chains, whose localized spins interact with conduction electrons via *sd* exchange interaction, to perform such comparison by starting from *unentangled* ground state of localized spins at the initial time. This reveals that quantum-classical dynamics can faithfully reproduce fully quantum dynamics in the FM case, but only when spin  $S$ , Heisenberg exchange between localized spins and *sd* exchange are sufficiently small. Increasing any of these three parameters can lead to substantial deviations, which are explained by the growth of *entanglement* between localized spins and/or between them and electrons. In the AFM case, substantial deviations appear even at early times, despite starting from *unentangled* Néel in equilibrium, which, therefore, poses a challenge on how to justify *rigorously* wide usage of the LL equation in modeling of antiferromagnetic spintronics experiments.

*Introduction.*—The development of consistent schemes for describing interaction of quantum and classical systems has been an interdisciplinary effort [1–7] due to great interest from both conceptual viewpoint and demands of practical calculations in physics and chemistry. Regarding the former, Copenhagen interpretation [8] of quantum mechanics crucially relies on measuring devices treated as classical objects which interact with a quantum system of interest [9]. Regarding the latter, in, e.g., chemical physics and chemistry it is impossible to numerically solve the Schrödinger equation for a macroscopically large number of particles, which is why a plethora of hybrid quantum-classical schemes have been developed [10, 11] where heavy particles (such as ions, atoms and molecules) are treated by classical molecular dynamics (MD) and only a much smaller number of lighter particles (such as electrons and protons [12, 13]) requires quantum dynamics that is (possibly nonadiabatically [13–15]) coupled to classical MD. Other examples that have motivated development of quantum-classical hybrid approaches include electrons interacting with nanoelectromechanical systems [16–18] or fast electronic spins interacting with slow classical local magnetization  $\mathbf{M}_i$  of magnetic materials [19, 20] embedded into spintronic devices [21–27]—in both cases electrons comprise a quantum system which is *open and out of equilibrium*.

Although a number studies have been focused on the general structure and properties of quantum-classical hybrid schemes, none are regarded as being the definitive solution. In the case of quantum electrons inter-

acting with classical localized spins, rigorous derivation of quantum-classical hybrid is bypassed, and one instead relies on celebrated Landau-Lifshitz (LL) equation

$$\frac{\partial \mathbf{S}_i}{\partial t} = -g \mathbf{S}_i \times \mathbf{B}_i^{\text{eff}} + \lambda \mathbf{S}_i \times \frac{\partial \mathbf{S}_i}{\partial t}, \quad (1)$$

introduced in 1935 [28] as a purely phenomenological one to treat localized spins  $\mathbf{S}_i$  (or, equivalently,  $\mathbf{M}_i \propto \mathbf{S}_i$ ) as classical vectors of fixed (unit,  $|\mathbf{S}| = 1$ ) length which can, therefore, only rotate. It has become the cornerstone of classical micromagnetics [29, 30] and classical atomistic spin dynamics [31] numerical schemes widely used to interpret [32] variety of experiments in contemporary research in spintronics and magnonics. The precessional term [first on the right-hand side in Eq. (1)]—where  $g$  is the gyromagnetic ratio; and  $\mathbf{B}_i^{\text{eff}} = -\frac{1}{\mu_M} \partial H_{\text{lspins}} / \partial \mathbf{S}_i$  is the effective magnetic field as the sum of external field, field due to interaction with other localized spins and magnetic anisotropy in the classical Hamiltonian of localized spins  $\mathcal{H}_{\text{lspins}}$ —can be derived from quantum mechanics [33]. The phenomenological damping term (second on the right-hand side in Eq. (1) and written originally [28] in a different “LL form” [34]) was justified by Gilbert [34] using the Lagrange formalism with the classical Rayleigh damping—it can also be derived microscopically but by starting [35] from a non-Hermitian Hamiltonian operator in order to take into account energy dissipation [34]. In all such quantum derivations of the LL equation, one constructs the Heisenberg equation of motion for the spin operators  $\hat{\mathbf{S}}_i$ , whose expectation values are then replaced (in the spirit of the Ehrenfest

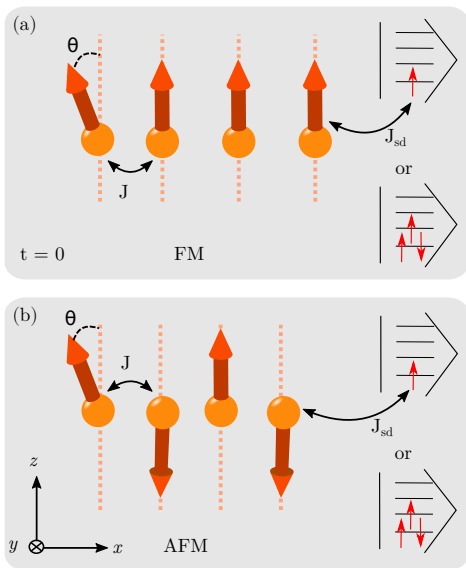


FIG. 1. Schematic view of 1D chains of  $N = 4$  sites  $i$  hosting quantum  $\hat{\mathbf{S}}_i$  or classical  $\mathbf{S}_i$  localized spins which interact via (a) NN ferromagnetic  $J > 0$  or (b) NN antiferromagnetic  $J < 0$  Heisenberg exchange. Conduction electrons hop between the sites, making 1D chains metallic, while their movable spins interact with localized spins via  $sd$  exchange interaction of strength  $J_{sd}$ . We use  $N_e = 1$  or  $N_e = 3$  electrons to fill the chain with their kets in the Fock space illustrated in the insets. The nonequilibrium dynamics is initiated by applying magnetic field locally at site  $i = 1$ ,  $B_1^x(t > 0) \neq 0$ . To enforce *unentangled* Néel state  $|\uparrow\downarrow \dots \uparrow\downarrow\rangle$  as the GS for  $t \leq 0$ , thereby making possible [35] comparison with classical [via Eq. (1)] modeling of localized spins, we employ the usual trick [39, 40]—staggered magnetic field  $B_i^z = -B_{i+1}^z$ .

theorem, which states that the expectation values obey the classical dynamical laws [36]) by classical vectors to finally arrive [33, 35] at Eq. (1). The Gilbert damping parameter  $\lambda$  is inserted “by hand,” from experiments [37] or from additional quantum calculations [38] employing single-electron Hamiltonian with spin-orbit or magnetic disorder scattering.

Although spin is a genuine internal quantum degree of freedom, it has been considered as a “rule of thumb” that spin dynamics becomes classical and amenable to description by the LL equation in the limit  $S \rightarrow \infty$  and  $\hbar \rightarrow 0$  (while  $S\hbar \rightarrow 1$ ). This is motivated by intuitive arguments, such as that the eigenvalue of  $\hat{\mathbf{S}}_i^2$  being  $S^2(1 + 1/S)$  suggests that quantum effects become progressively less important for  $S > 1$ . However, they actually persist for all  $S < \infty$ , vanishing as  $1/2S$  in the classical limit [41]. Furthermore, in contrast to chemical physics and chemistry where many nuclei are much heavier than electrons so that classical MD safely applies to them [12], most of standard magnetic materials host localized spins  $S \leq 5/2$  [42]. This issue has ignited intense efforts [33, 35, 43, 44] to delineate the limits of appli-

cability of the LL equation by directly comparing quantum  $\langle \hat{\mathbf{S}}_i \rangle(t)$  vs. classical  $\mathbf{S}_i(t)$  [computed by LL equation but without damping term in Eq. (1)] trajectories and their Fourier transforms [44] for systems of localized spins *alone* in models of FM insulators.

Such studies of a *single* localized spin have revealed [33, 44] that the presence of terms quadratic in  $\hat{\mathbf{S}}_i$ , such as due to magnetic anisotropy  $D_z(\hat{S}_i^z)^2$  or biquadratic exchange  $J_b(\hat{\mathbf{S}}_i \cdot \hat{\mathbf{S}}_j)^2$ , makes quantum and classical trajectories substantially different for small  $S$ . Although the discrepancy can be reduced by increasing  $S$  to very large values [44], this works only for finite time interval (which elongates with  $S \rightarrow \infty$ ) because of always present quantum revivals [44]. This finding is not surprising in the light of the breakdown [36] of the Ehrenfest theorem for any nonlinear potential  $V(\hat{\mathbf{r}})$  because  $\langle \hat{\mathbf{r}}^p \rangle \neq (\hat{\mathbf{r}})^p$  when  $p > 2$ .

For *many* localized spins, a more demanding requirement for applicability of coupled LL equations, coded in all modern classical micromagnetics [29, 30] and atomistic spin dynamics codes [31], is that their quantum many-body state *must* [35] remain *unentangled or separable* [45–47],  $|\Sigma(t)\rangle_{\text{ispins}} = |\sigma_1(t)\rangle \otimes |\sigma_2(t)\rangle \otimes \dots \otimes |\sigma_N(t)\rangle$ , for all times  $t$ . Otherwise, if one starts from unentangled states, such as the ground state (GS) of a ferromagnet (FM)  $|\text{GS}\rangle_{\text{FM}} = |\uparrow\uparrow \dots \uparrow\uparrow\rangle$ , but their superpositions and thereby entanglement are created dynamically [47], one finds that vector magnitude  $|\langle \hat{\mathbf{S}}_i(t) \rangle| < S\hbar$  is shrinking (sometimes even to zero [47]) as the entanglement increases in time. This is a genuine quantum effect that cannot be mimicked by any classical equation [35]. In addition, in the case of antiferromagnets (AFMs), the true GS is always substantially different from unentangled Néel state  $|\Sigma\rangle_{\text{ispins}}^{\text{Néel}} = |\uparrow\downarrow \dots \uparrow\downarrow\rangle$  (always assumed when using classical atomistic spin dynamics codes [31]), with entanglement present in equilibrium and, therefore, at  $t = 0$  [48–50]. For example, in the minimalistic [Fig. 1(b)] system of four localized spins  $S = 1/2$  interacting with the nearest-neighbor (NN) Heisenberg exchange  $J < 0$ , the true GS is  $|\text{GS}\rangle_{\text{AFM}} = \frac{1}{\sqrt{12}}(2|\uparrow\downarrow\uparrow\downarrow\rangle + 2|\downarrow\uparrow\downarrow\uparrow\rangle - |\uparrow\uparrow\downarrow\downarrow\rangle - |\uparrow\downarrow\downarrow\uparrow\rangle - |\downarrow\downarrow\uparrow\uparrow\rangle - |\downarrow\uparrow\uparrow\downarrow\rangle)$ , ensuring lower energy  $\langle \text{GS} | \hat{H}_{\text{AFM}} | \text{GS} \rangle = 2J$  than the energy in the unentangled Néel state,  $\langle \uparrow\downarrow\uparrow\downarrow | \hat{H}_{\text{AFM}} | \uparrow\downarrow\uparrow\downarrow \rangle = J$ . While  $\langle \uparrow\downarrow\uparrow\downarrow | \hat{\mathbf{S}}_i | \uparrow\downarrow\uparrow\downarrow \rangle = \pm S\hbar$ , in the true GS expectation values of localized spins are  ${}_{\text{AFM}}\langle \text{GS} | \hat{\mathbf{S}}_i | \text{GS} \rangle_{\text{AFM}} \equiv 0$  akin to any quantum spin liquid [51].

Despite these insights, *no comparison exists* fully quantum many-body vs. quantum-classical nonequilibrium dynamics for a system of localized spins interacting with conduction electrons. This is largely due to the fact that self-consistent quantum-classical schemes have been developed only very recently [21–27], in contrast to earlier efforts [52–55] attempting to “integrate out” fast electrons and arrive at effective *spin-only* (i.e., of extended LL type [22, 25]) equations which can never succeed [22, 25] in all relevant parameter regimes.

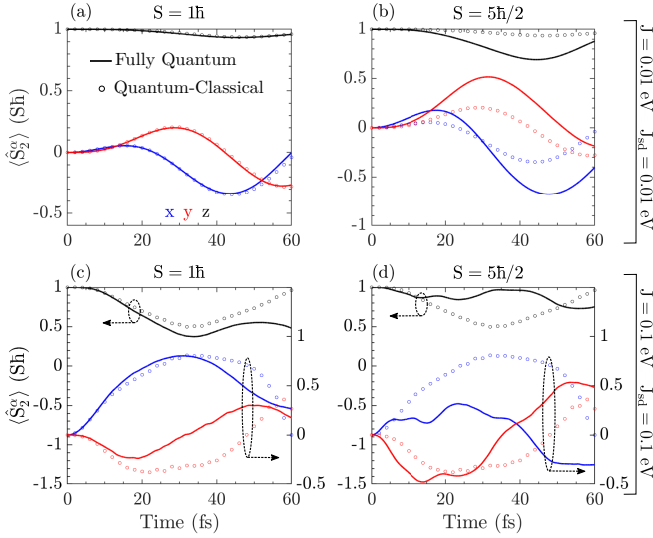


FIG. 2. Time evolution of localized spin at site  $i = 2$  within FM chain [Fig. 1(a)] from fully quantum (solid lines) vs. quantum-classical (open circles) calculations. Two different localized spins ( $S = 1$  and  $S = 5/2$ ) are used in fully quantum calculations, while quantum-classical calculations treat localized spins as unit vectors of fixed length  $|\mathbf{S}_i| = 1$ . We also use two different sets of parameters [shown on the right for panels (a),(b) vs. panels (c),(d)] for Heisenberg and  $sd$  exchange interaction between localized spins and electron spin and localized spins, respectively.

In this Letter, we choose small FM or AFM chains of  $N = 4$  spins  $S = 1$  or  $S = 5/2$ , which interact via the NN Heisenberg exchange  $J$  and are localized on lattice sites between which conduction electrons can hop while their movable spins interact with localized spins via  $sd$  exchange coupling of strength  $J_{sd}$ , as illustrated in Fig. 1. These chains mimic essential features of FM or AFM metallic elements within spintronic devices, while their relatively small Hilbert space of dimension  $4^N(2S+1)^N$  makes possible numerically exact treatment [56]. In fact, short FM [57] and AFM [58] chains have been realized experimentally using artificial chains of Fe atoms on a substrate. Prior to explaining our principal results in Figs. 2–4—comparing quantum-classical trajectories  $\mathbf{S}_i(t)$  to fully quantum trajectories  $\langle \hat{\mathbf{S}}_i \rangle(t)$  in FM [Fig. 2] and AFM [Fig. 4] while connecting any deviation between them to the growth of entanglement [Figs. 3 and 4(d)], we first introduce useful concepts and notation.

*Models and methods.*—The FM and AFM models in Fig. 1 are described by quantum many-body Hamiltonian

$$\hat{H} = \hat{H}_{\text{spins}} + \hat{H}_e + \hat{H}_{e-\text{spins}}(t > 0) + \hat{H}_{\mathbf{B}} \quad (2)$$

acting in  $\mathcal{H}_{\text{total}} = \mathcal{F}_e \otimes \mathcal{H}_1 \otimes \cdots \otimes \mathcal{H}_4$  as the tensor product of the Fock space  $\mathcal{F}_e$  for electrons and Hilbert spaces  $\mathcal{H}_i$  for localized spins. The localized spins are described by the quantum Heisenberg Hamiltonian,  $\hat{H}_{\text{spins}} = -J \sum_{\langle ij \rangle} \hat{\mathbf{S}}_i \cdot \hat{\mathbf{S}}_j$ , where  $\langle ij \rangle$  indicates interaction between the NN sites. Here the spin operator

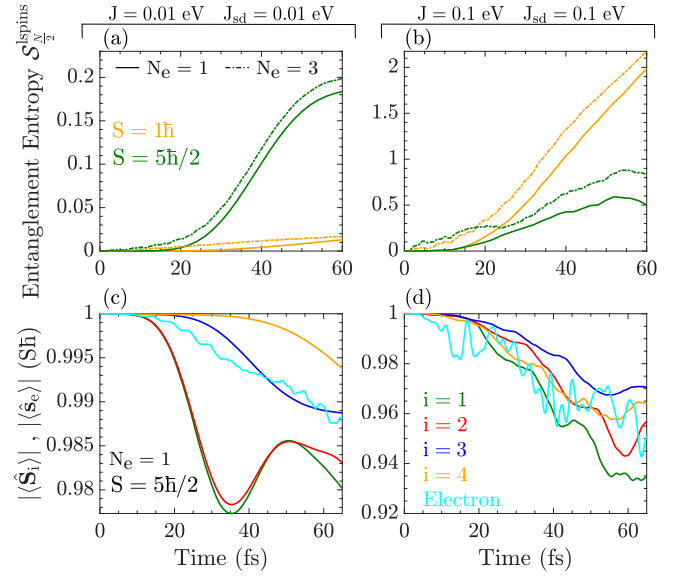


FIG. 3. (a) and (b) Time evolution of the von Neumann entanglement entropy [45] for the subsystem of FM chain [Fig. 1(a)], composed of half [46, 47] of all localized spins (that is at sites  $i = 3, 4$ ), which is extracted from fully quantum time evolution of the whole system of electrons and localized spins studied in Fig. 2. Cases with  $N_e = 1$  (solid lines) and  $N_e = 3$  (dash-dot lines) conduction electrons filling the chain are considered. Panels (c) and (d) show time evolution of the magnitude of the expectation values of localized spins and electron spin, in the case  $S = 5/2$  and  $N_e = 1$ , whose decay below one (such as  $|\langle \hat{\mathbf{S}}_i \rangle(t)|/S\hbar < 1$  and  $|\langle \hat{\mathbf{s}}_e \rangle(t)|/2\hbar < 1$ ) signifies growth of entanglement [46, 47] of such minimal subsystem with the rest of the total system.

$\hat{S}_i^\alpha = \underbrace{\mathbb{1} \otimes \mathbb{1} \cdots \mathbb{1}}_{i-1} \otimes \hat{S}^\alpha \otimes \underbrace{\mathbb{1} \otimes \mathbb{1} \cdots \mathbb{1}}_{N-i \text{ times}}$  at site  $i$  is a matrix of size  $(2S+1)^N$  for spin  $S$ , where  $\mathbb{1}$  is unit matrix of size  $(2S+1)$ . The tight-binding Hamiltonian for conduction electrons is  $\hat{H}_e = -\gamma \sum_{\langle ij \rangle, \sigma} \hat{c}_{i\sigma}^\dagger \hat{c}_{j\sigma}$ , where  $\gamma = 1 \text{ eV}$  (setting the unit of energy) is the NN hopping between  $s$ -orbitals centered on each site  $i$ . Here  $\hat{c}_{i\sigma}^\dagger$  ( $\hat{c}_{i\sigma}$ ) creates (annihilates) an electron with spin  $\sigma = \uparrow, \downarrow$  on site  $i$ , so that each site can host one of the four possible electronic states obeying the Pauli principle—empty  $|0\rangle$ , spin-up  $\hat{c}_{i\uparrow}^\dagger|0\rangle$ , spin-down  $\hat{c}_{i\downarrow}^\dagger|0\rangle$ , and doubly occupied  $\hat{c}_{i\uparrow}^\dagger \hat{c}_{i\downarrow}^\dagger|0\rangle$ . The interaction between conduction electron spin and localized spin is described by  $sd$  (in common spintronics terminology) Hamiltonian,  $\hat{H}_{e-\text{spins}} = -J_{sd}(t > 0) \sum_{i=1}^N \hat{\mathbf{s}}_i \cdot \hat{\mathbf{S}}_i$ , where  $\hat{s}_i^\alpha = \sum_{\sigma, \sigma' = \{\uparrow, \downarrow\}} \hat{c}_{i\sigma}^\dagger \hat{\sigma}_{\sigma\sigma'}^\alpha \hat{c}_{i\sigma'}$  is the local (per-site) spin density operators;  $\hat{\sigma}^\alpha$  is the Pauli matrix; and  $\hat{s}_e^\alpha = \sum_{i=1}^N \hat{s}_i^\alpha$  is then the operator of the total electron spin along the  $\alpha$ -axis. Note that the same  $sd$  Hamiltonian, together with first two terms in Eq. (2), is termed Kondo-Heisenberg model in the physics of strongly correlated electrons [59]. The last Zeeman term in Eq. (2) is due to externally applied magnetic

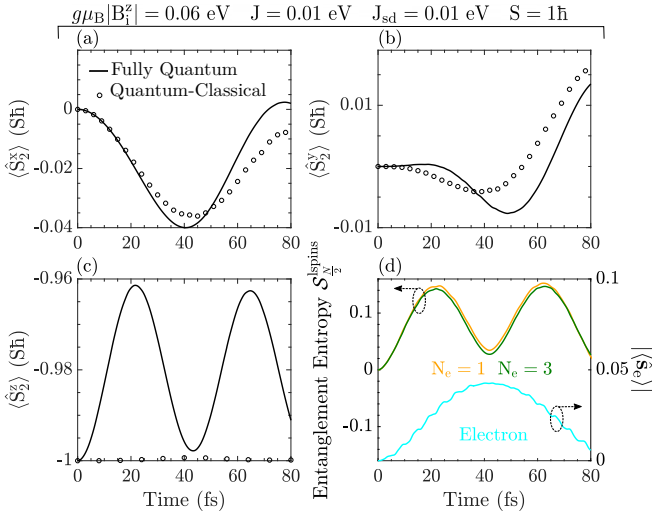


FIG. 4. (a)–(c) Time evolution of localized spin at site  $i = 2$  within AFM chain [Fig. 1(b)] from fully quantum (solid lines) vs. quantum-classical (open circles) calculations. The quantum localized spin is  $S = 1$  in fully quantum calculations, while quantum-classical calculations treat localized spins as unit vectors of fixed length  $|\mathbf{S}_i| = 1$ . We also use two different sets of parameters [shown on the right for panels (a),(b) vs. panels (c),(d)] for Heisenberg and  $sd$  exchange interaction between localized spins and electron spin and localized spins, respectively. Panel (d) shows the entanglement entropy for half ( $i = 3, 4$ ) of all localized spins in the case with  $N_e = 1$  or  $N_e = 3$  electrons, as well as the magnitude of the expectation value of electron spin in the case  $N_e = 1$ .

fields,  $\hat{H}_{\mathbf{B}} = -g\mu_B \sum_{i=1}^N B_i^z \hat{S}_i^z - g\mu_B B_1^x(t > 0) \hat{S}_1^x$ . In the case of FM [Fig. 1(a)],  $g\mu_B B_i^z = 0.1$  eV ( $\mu_B$  is the Bohr magneton) acts as anisotropy to select the positive  $z$ -axis as the easy axis, and  $g\mu_B B_1^x(t > 0) = 0.1$  eV is applied at first site  $i = 1$  to initiate [35] nonequilibrium dynamics for  $t > 0$ . In the case of AFM [Fig. 1(b)], we apply staggered field  $B_i^z = -B_{i+1}^z$  of magnitude  $g\mu_B |B_i^z| = 0.06$  eV for all times to select (since  $g\mu_B |B_i^z| > J$ ) the Néel state as the GS with no entanglement for  $t \leq 0$ , while  $g\mu_B B_1^x(t > 0) = 0.01$  eV initiates nonequilibrium dynamics.

In fully quantum dynamics, wavefunction of isolated quantum many-body system electrons+localized-spins is evolved within  $\mathcal{H}_{\text{total}}$  using  $|\Psi(t + \delta t)\rangle = \mathcal{T} \exp\left(-\frac{i}{\hbar} \int_t^{t+\delta t} \hat{H}(t)\right) |\Psi(t)\rangle$ , where  $\mathcal{T}$  is the time ordering operator and we employ the Crank-Nicolson algorithm [60] with time step  $\delta t = 0.01$  fs. The initial state  $|\Psi(t = 0)\rangle = |\chi(t = 0)\rangle_e \otimes |\Sigma(t = 0)\rangle_{\text{lspins}}$  is unentangled GS, whose factor  $|\Sigma\rangle_{\text{lspins}}$  for localized spins is also unentangled ( $|\Sigma(t = 0)\rangle_{\text{lspins}} = |\uparrow\uparrow \dots \uparrow\uparrow\rangle$  for FM or  $|\Sigma(t = 0)\rangle_{\text{lspins}}^{\text{Néel}} = |\uparrow\downarrow \dots \uparrow\downarrow\rangle$ ) as a prerequisite [35] for compare quantum vs. classical dynamics of localized spins. The unentangled GS is ensured by switching on  $sd$  Hamiltonian  $\hat{H}_{e-\text{lspins}}(t > 0)$  in Eq. (2) at  $t = 0$  since

GS would otherwise be entangled [56] with entanglement entropy  $\mathcal{S}_N^{\text{lspins}} = \mathcal{S}_e \simeq 10^{-3}$ . The von Neumann entanglement entropy [45–47] of a chosen subsystem is computed as  $\mathcal{S}_{\text{sub}}(t) = -\text{Tr}[\hat{\rho}(t)_{\text{sub}} \log_2 \hat{\rho}(t)_{\text{sub}}]$  using the reduced density matrix,  $\hat{\rho}(t)_{\text{sub}} = \text{Tr}_{\text{other}} |\Psi(t)\rangle \langle \Psi(t)|$ , obtained by partial trace of pure state density matrix over all other degrees of freedom. Note that when total system is split into two parts, they have identical entropies, such as  $\mathcal{S}_N^{\text{lspins}} = \mathcal{S}_e$ .

In quantum-classical description of the same system, we switch to classical Hamiltonian

$$H_{\text{lspins}} = -J \sum_{\langle ij \rangle} \mathbf{S}_i \cdot \mathbf{S}_j - J_{sd} \sum_{i=1}^N \langle \hat{\mathbf{s}}_i^e \rangle(t) \cdot \mathbf{S}_i + H_{\mathbf{B}}, \quad (3)$$

for localized spins  $\mathbf{S}_i$  where  $H_{\mathbf{B}}$  is classical version of  $\hat{H}_{\mathbf{B}}$  in Eq. (2). The quantum Hamiltonian for electrons then retains only two terms from  $\hat{H}$  in Eq. (2),  $\hat{H}(t) = \hat{H}_e - J_{sd} \sum_{i=1}^N \hat{\mathbf{s}}_i \cdot \mathbf{S}_i(t)$ , with its time-dependence being generated by self-consistent coupling at each time step to  $\mathbf{S}_i(t)$  obtained by solving the LL equation. When solving the LL equation we set Gilbert damping  $\lambda = 0$  in Eq. (1), as also used in previous comparisons [33, 35, 43, 44] of quantum vs. classical dynamics for localized spins *alone*. This choice is due to their quantum calculations handling FM insulator, or ours handling FM or AFM metal, which are considered as being isolated quantum systems that are not coupled to natural intrinsic bosonic baths (such as phonons of the crystal lattice or photons of the ambient electromagnetic environment), external baths [27] or external fermionic reservoirs [21–24, 26] all of which contain an infinite number of degrees of freedom thereby supplying continuous energy spectrum. Nevertheless, our calculations are still qualitatively different from those of Refs. [33, 35, 43, 44] because excitation energy and excess spin are transported away from localized spins by *nonequilibrium* conduction electrons driven out of equilibrium by time dependence of  $\mathbf{S}_i(t)$ . While this effect is often modeled by adding spin-transfer torque (STT),  $\frac{g}{\mu_M} \mathbf{T}_i [\mathbf{S}_i(t)]$ , into the LL equation as electronic back-action [23, 24, 61–63], in our quantum-classical calculations it is automatically included by self-consistent loop where such term can be nonlocal in space [23, 24] and time [22, 25]. Besides conventional Slonczewski-Berger [19, 29] STT  $\mathbf{T}_i [\mathbf{S}_i(t)] \propto \langle \hat{\mathbf{s}}_i^e \rangle(t) \times \mathbf{S}_i(t)$ , our fully quantum calculation also include quantum STT [40, 47, 48, 64] where transfer of spin angular momentum between electrons and localized spins is possible even when  $\langle \hat{\mathbf{s}}_i^e \rangle$  is *collinear but antiparallel* [47] to the direction of  $\langle \hat{\mathbf{S}}_i \rangle$ .

*Results and discussion.*—Let us first recall [24, 63] that electronic hopping  $\gamma$  and  $sd$  exchange  $J_{sd}$  control the speed of electron translational and spin dynamics, respectively—e.g., large ratio  $J_{sd}/\gamma$  is required to bring the system of conduction electrons and localized spins into “adiabatic limit” where electron spin remains in

the lowest energy state at each time while locking to the direction of localized spins. Figure 2(a),(b) shows that small  $J$  and  $J_{sd}$  make possible for quantum-classical trajectories  $\mathbf{S}_i(t)$  to re-trace fully quantum trajectories  $\langle \hat{\mathbf{S}}_i \rangle(t)$  in FM metallic chain [Fig. 1(a)] over long time intervals, but this correspondence is lost by increasing  $J$  and  $J_{sd}$  [Fig. 2(c),(d)]. Surprisingly, in contrast to “rule of thumb” arguments [29–31, 41] and previous rigorous comparisons [33, 35, 43, 44] of quantum vs. classical trajectories of localized spins in the *absence* of conduction electrons—where increasing  $S \rightarrow \infty$  justifies applicability of the LL equation—increasing localized spins from  $S = 1$  [Fig. 2(a),(c)] to  $S = 5/2$  [Fig. 2(b),(d)] leads to large deviations between  $\mathbf{S}_i(t)$  and  $\langle \hat{\mathbf{S}}_i \rangle(t)$ . We explain emergence of such large deviations as a function of time by the growth of entanglement entropy of localized spin subsystem [Fig. 3], which is enabled by increasing  $J_{sd}$  that facilitates entangling localized spins to conduction electrons; or increasing  $S$ , which enlarges the environment to which individual [Fig. 3(c),(d)] localized spins or electronic spin can entangle. Since entanglement is a genuine quantum phenomenon, as soon as it becomes nonzero the magnitude of vectors  $|\langle \hat{\mathbf{S}}_i \rangle(t)| < S\hbar$  shrinks [Fig. 3(c),(d)] making the LL equation *inapplicable* [35].

For AFM metallic chain [Fig. 1(b)], large deviations in Fig. 4 between  $\mathbf{S}_i(t)$  and  $\langle \hat{\mathbf{S}}_i \rangle(t)$  are present from the outset  $t \gtrsim 0$ , despite using: (i) unentangled Néel state  $|\Sigma\rangle_{\text{lspins}}^{\text{Néel}}$  as the initial condition at  $t = 0$ ; and (ii) small values  $S = 1$ ,  $J$  and  $J_{sd}$ , which in the case of FM chain ensure [Fig. 2(a)] good match between quantum-classical and fully quantum trajectories. This is explained by much more rapid increase of entanglement entropy of localized spins for  $t \gtrsim 0$  in the AFM case [Fig. 4(d)] than in the FM case [Fig. 3(a),(b)]. Note that in both FM and AFM cases, increasing the number of conduction electrons from  $N_e = 1$ , where  $|\chi(t = 0)\rangle_e = \hat{c}_{1\uparrow}^\dagger|0\rangle$ ; to  $N_e = 3$ , where  $|\chi(t = 0)\rangle_e = \hat{c}_{1\uparrow}^\dagger\hat{c}_{1\downarrow}^\dagger\hat{c}_{2\uparrow}^\dagger|0\rangle$ , leads to similar entanglement entropies [Figs. 3(a),(b) and 4(d)] and trajectories (not shown explicitly) of  $\langle \hat{\mathbf{S}}_i \rangle(t)$  because  $|\langle \hat{\mathbf{S}}_e \rangle(t = 0)| = \hbar/2$  in both  $N_e = 1$  and  $N_e = 3$  cases.

*Conclusions ant outlook.*—The quantum-classical and fully quantum-many-body computed trajectories of localized spins in FM metal, where they interact with conduction electrons, can be matched in some parameter regimes and time intervals [Figs. 2 and 3], akin to previous analogous comparisons [33, 35, 43, 44] but in FM insulators *without* conduction electrons. However, in sharp contrast to these studies, two types of trajectories deviate more (rather than less as in Refs. [33, 35, 43, 44]) from each other with increasing  $S$  of localized spins. Furthermore, no match is found whatsoever in the case of AFM metal, which casts a doubt on applicability of phenomenological theories [65] [based on LL Eq. (1)] widely used in antiferromagnetic spintronics [20]. The doubt could be resolved by identifying (which we re-

gate for future studies) decoherence channels due to environment outside of electronic and localized spins subsystems, which can disrupt superpositions of quantum many-body states and maintain entanglement entropy of localized spins [Fig. 4(d)] *close to zero* for all times so that nonclassical effects (like entanglement, which the LL equation can never capture) are *suppressed*.

This work was supported by the U.S. National Science Foundation (NSF) Grant No. ECCS 1922689.

---

\* bnkolic@udel.edu

- [1] M. V. Berry and J. M. Robbins, Chaotic classical and half-classical adiabatic reactions: geometric magnetism and deterministic friction, Proc. R. Soc. Lond. A **442**, 659 (1993).
- [2] Q. Zhang and B. Wu, General approach to quantum-classical hybrid systems and geometric forces, Phys. Rev. Lett. **97**, 190401 (2006).
- [3] F. Agostini, S. Caprara and G. Ciccotti, Do we have a consistent non-adiabatic quantum-classical mechanics?, EPL (Europhysics Letters) **78**, 30001 (2007).
- [4] H.-T. Elze, Linear dynamics of quantum-classical hybrids, Phys. Rev. A **85**, 052109 (2012).
- [5] M. Radonjić, S. Prvanović, and N. Burić, Hybrid quantum-classical models as constrained quantum systems, Phys. Rev. A **85**, 064101 (2012).
- [6] C. Barceló, R. Carballo-Rubio, L. J. Garay, R. Gómez-Escalante, Hybrid classical-quantum formulations ask for hybrid notions, Phys. Rev. A **86**, 042120 (2012).
- [7] T. A. Oliynyk, Classical-quantum limits, Found. Phys. **46**, 1551 (2016).
- [8] C. Rovelli, Relational quantum mechanics, Int. J. of Theor. Phys. **35**, 1637 (1996).
- [9] H. Nikolić, Internal environment: what is it like to be a Schrödinger cat?, Eur. J. Phys. **36**, 045003 (2015).
- [10] R. Kapral, Progress in the theory of mixed quantum-classical dynamics, Annu. Rev. Phys. Chem. **57**, 129 (2006).
- [11] R. Kapral, Quantum dynamics in open quantum-classical systems, J. Phys.: Condens. Matter **27**, 073201 (2015).
- [12] T. E. Markland and M. Ceriotti, Nuclear quantum effects enter the mainstream, Nat. Rev. Chem. **2**, 0109 (2018).
- [13] L. Kantorovich, Nonadiabatic dynamics of electrons and atoms under nonequilibrium conditions, Phys. Rev. B **98**, 014307 (2018).
- [14] F. Agostini and B. F. E. Curchod, Different flavors of nonadiabatic molecular dynamics, WIREs Comput. Mol. Sci. **9**, e1417 (2019).
- [15] W. Dou and J. E. Subotnik, Perspective: How to understand electronic friction, J. Chem. Phys. **148**, 230901 (2018).
- [16] N. Bode, S. V. Kusminskiy, R. Egger, and F. von Oppen, Scattering theory of current-induced forces in mesoscopic systems, Phys. Rev. Lett. **107**, 036804 (2011).
- [17] M. Thomas, T. Karzig, S. V. Kusminskiy, G. Zaránd, and F. von Oppen, Scattering theory of adiabatic reaction forces due to out-of-equilibrium quantum environments, Phys. Rev. B **86**, 195419 (2012).
- [18] J.-T. Lü, M. Brandbyge, P. Hedegård, T. N. Todorov,

- and D. Dundas, Current-induced atomic dynamics, instabilities, and Raman signals: Quasiclassical Langevin equation approach, *Phys. Rev. B* **85**, 245444 (2012).
- [19] D. Ralph and M. Stiles, Spin transfer torques, *J. Magn. Mater.* **320**, 1190 (2008).
- [20] V. Baltz, A. Manchon, M. Tsoi, T. Moriyama, T. Ono, and Y. Tserkovnyak, Antiferromagnetic spintronics, *Rev. Mod. Phys.* **90**, 015005 (2018).
- [21] M. D. Petrović, B. S. Popescu, U. Bajpai, P. Plecháč, and B. K. Nikolić, Spin and charge pumping by a steady or pulse-current-driven magnetic domain wall: A self-consistent multiscale time-dependent quantum-classical hybrid approach, *Phys. Rev. Applied* **10**, 054038 (2018).
- [22] U. Bajpai and B. K. Nikolić, Time-retarded damping and magnetic inertia in the Landau-Lifshitz-Gilbert equation self-consistently coupled to electronic time-dependent nonequilibrium Green functions, *Phys. Rev. B* **99**, 134409 (2019).
- [23] U. Bajpai and B. K. Nikolić, Spintronics meets nonadiabatic molecular dynamics: Geometric spin torque and damping on dynamical classical magnetic texture due to an electronic open quantum system, *Phys. Rev. Lett.* **125**, 187202 (2020).
- [24] M. D. Petrović, U. Bajpai, P. Plecháč, and B. K. Nikolić, Annihilation of topological solitons in magnetism with spin wave burst finale: The role of nonequilibrium electrons causing nonlocal damping and spin pumping over ultrabroadband frequency range, *Phys. Rev. B* **104**, L020407 (2021).
- [25] M. Sayad and M. Potthoff, Spin dynamics and relaxation in the classical-spin Kondo-impurity model beyond the Landau-Lifshitz-Gilbert equation, *New J. Phys.* **17**, 113058 (2015).
- [26] E. V. Boström and C. Verdozzi, Steering magnetic skyrmions with currents: A nonequilibrium Green's functions approach, *Phys. Stat. Solidi B* **256**, 1800590 (2019).
- [27] M. Elbracht and M. Potthoff, Accessing long timescales in the relaxation dynamics of spins coupled to a conduction-electron system using absorbing boundary conditions, *Phys. Rev. B* **102**, 115434 (2020).
- [28] L. D. Landau and E. M. Lifshitz, On the theory of the dispersion of magnetic permeability in ferromagnetic bodies, *Phys. Z. Sowjetunion* **8**, 153 (1935).
- [29] D. V. Berkov and J. Miltat, Spin-torque driven magnetization dynamics: Micromagnetic modeling, *J. Magn. Mater.* **320**, 1238 (2008).
- [30] S.-K. Kim, Micromagnetic computer simulations of spin waves in nanometre-scale patterned magnetic elements, *J. Phys. D: Appl. Phys* **43**, 264004 (2010).
- [31] R. F. L. Evans, W. J. Fan, P. Chureemart, T. A. Ostler, M. O. A. Ellis, and R. W. Chantrell, Atomistic spin model simulations of magnetic nanomaterials, *J. Phys.: Condens. Matter* **26**, 103202 (2014).
- [32] S. Woo, T. Delaney, and G. S. D. Beach, Magnetic domain wall depinning assisted by spin wave bursts, *Nat. Phys.* **13**, 448 (2017).
- [33] R. Weiser, Role of quadratic terms in the Heisenberg model for quantum spin dynamics, *Phys. Rev. B* **84**, 054411 (2011).
- [34] W. M. Saslow, Landau-Lifshitz or Gilbert damping? That is the question, *J. Appl. Phys.* **105**, 07D315 (2009).
- [35] R. Wieser, Description of a dissipative quantum spin dynamics with a Landau-Lifshitz/Gilbert like damping and complete derivation of the classical Landau-Lifshitz equation, *Euro. Phys. J. B* **88**, 77 (2015).
- [36] L. E. Ballentine, Y. Yang, and J. P. Zibin, Inadequacy of Ehrenfest's theorem to characterize the classical regime, *Phys. Rev. A* **50**, 2854 (1994).
- [37] T. Weindler, H. G. Bauer, R. Islinger, B. Boehm, J.-Y. Chauleau, and C. H. Back, Magnetic damping: Domain wall dynamics versus local ferromagnetic resonance, *Phys. Rev. Lett.* **113**, 237204 (2014).
- [38] A. A. Starikov, P. J. Kelly, A. Brataas, Y. Tserkovnyak, and G. E. W. Bauer, Unified first-principles study of Gilbert damping, spin-flip diffusion, and resistivity in transition metal alloys, *Phys. Rev. Lett.* **105**, 236601 (2010).
- [39] E. M. Stoudenmire and S. R. White, Studying two-dimensional systems with the density matrix renormalization group, *Annu. Rev. Condens. Matter Phys.* **3**, 111 (2012).
- [40] A. Mitrofanov and S. Urazhdin, Nonclassical spin transfer effects in an antiferromagnet, *Phys. Rev. Lett.* **126**, 037203 (2021).
- [41] J. B. Parkinson, J. C. Bonner, G. Müller, M. P. Nightingale, and H. W. J. Blüte, Heisenberg spin chains: Quantum-classical crossover and the Haldane conjecture, *J. Appl. Phys.* **57**, 3319 (1985).
- [42] E. Kaxiras and J. D. Joannopoulos, *Quantum Theory of Materials* (Cambridge University Press, Cambridge, 2019).
- [43] R. Wieser, Comparison of quantum and classical relaxation in spin dynamics, *Phys. Rev. Lett.* **110**, 147201 (2013).
- [44] J. P. Gauyacq and N. Lorente, Classical limit of a quantum nano-magnet in an anisotropic environment, *Surf. Sci.* **630**, 325 (2014).
- [45] G. De Chiara and A. Sanpera, Genuine quantum correlations in quantum many-body systems: a review of recent progress, *Rep. Prog. Phys.* **81**, 074002 (2018).
- [46] J. H. Bardarson, F. Pollmann, and J. E. Moore, Unbounded growth of entanglement in models of many-body localization, *Phys. Rev. Lett.* **109**, 017202 (2012).
- [47] M. D. Petrović, P. Mondal, A. E. Feiguin, P. Plecháč, and B. K. Nikolić, Spintronics meets density matrix renormalization group: Quantum spin-torque-driven nonclassical magnetization reversal and dynamical buildup of long-range entanglement, *Phys. Rev. X* **11**, 021062 (2021).
- [48] M. D. Petrović, P. Mondal, A. E. Feiguin, and B. K. Nikolić, Quantum spin torque driven transmutation of an antiferromagnetic Mott insulator, *Phys. Rev. Lett.* **126**, 197202 (2021).
- [49] N. B. Christensen, H. M. Rønnow, D. F. McMorrow, A. Harrison, T. G. Perring, M. Enderle, R. Coldea, L. P. Regnault, and G. Aeppli, Quantum dynamics and entanglement of spins on a square lattice, *PNAS* **104**, 15264 (2007).
- [50] A. Kamra, E. Thingstad, G. Rastelli, R. A. Duine, A. Brataas, W. Belzig, and A. Sudbø, Antiferromagnetic magnons as highly squeezed Fock states underlying quantum correlations, *Phys. Rev. B* **100**, 174407 (2019).
- [51] C. Broholm, R. J. Cava, S. A. Kivelson, D. G. Nocera, M. R. Norman, and T. Senthil, Quantum spin liquids, *Science* **367**, 263 (2020).
- [52] M. Onoda and N. Nagaosa, Dynamics of localized spins coupled to the conduction electrons with charge and spin currents, *Phys. Rev. Lett.* **96**, 066603 (2006).
- [53] A. S. Núñez and R. A. Duine, Effective temperature and

- Gilbert damping of a current-driven localized spin, *Phys. Rev. B* **77**, 054401 (2008).
- [54] J. Fransson and J.-X. Zhu, Spin dynamics in a tunnel junction between ferromagnets, *New J. Phys.* **10**, 013017 (2008).
- [55] H. M. Hurst, V. Galitski, and T. T. Heikkilä, Electron-induced massive dynamics of magnetic domain walls, *Phys. Rev. B* **101**, 054407 (2020).
- [56] U. Bajpai, A. Suresh, and B. K. Nikolić, Quantum many-body states and Green functions of nonequilibrium electron-magnon systems: Localized spin operators vs. their mapping to Holstein-Primakoff bosons, [arXiv:2104.07657](https://arxiv.org/abs/2104.07657) (2021).
- [57] A. Spinelli, B. Bryant, F. Delgado, J. Fernández-Rossier, and A. F. Otte, Imaging of spin waves in atomically designed nanomagnets, *Nat. Mater.* **10**, 782 (2014).
- [58] S. Loth, S. Baumann, C. P. Lutz, D. M. Eigler, and A. J. Heinrich, Bistability in atomic-scale antiferromagnets, *Science* **335**, 196 (2012).
- [59] A. M. Tsvetik and O. M. Yevtushenko, Chiral spin order in Kondo-Heisenberg systems, *Phys. Rev. Lett.* **119**, 247203 (2017).
- [60] D. Wells and H. Quiney, A fast and adaptable method for high accuracy integration of the time-dependent Schrödinger equation, *Sci. Rep.* **9**, 782 (2019).
- [61] S. Zhang and Z. Li, Roles of nonequilibrium conduction electrons on the magnetization dynamics of ferromagnets, *Phys. Rev. Lett.* **93**, 127204 (2004).
- [62] S. Zhang and S. S.-L. Zhang, Generalization of the Landau-Lifshitz-Gilbert equation for conducting ferromagnets, *Phys. Rev. Lett.* **102**, 086601 (2009).
- [63] G. Tatara, Effective gauge field theory of spintronics, *Physica E* **106**, 208 (2019).
- [64] A. Zholud, R. Freeman, R. Cao, A. Srivastava, and S. Urazhdin, Spin transfer due to quantum magnetization fluctuations, *Phys. Rev. Lett.* **119**, 257201 (2017).
- [65] K. M. D. Hals, Y. Tserkovnyak, and A. Brataas, Phenomenology of current-induced dynamics in antiferromagnets, *Phys. Rev. Lett.* **106**, 107206 (2011).